Diffusion and Electrical Properties of Boron and Arsenic Doped Poly-Si and Poly-Ge_xSi_{1-x} ($x \sim 0.3$) as Gate Material for Sub-0.25 μm Complementary Metal Oxide Semiconductor Applications

C. Salm,[a] D. T. van Veen,[a] D. J. Gravesteijn,[b] J. Holleman,*[,a] and P. H. Woerlee[a,b]

[a] *MESA Research Institute, University of Twente, 7500 AE Enschede, The Netherlands*
[b] *Philips Research Laboratories, Eindhoven, The Netherlands*

ABSTRACT

In this paper the texture, morphology, diffusion and electrical (de-) activation of dopants in polycrystalline Ge_xSi_{1-x} and Si have been studied in detail. For gate doping B^+, BF_2^+, and As^+ were used and thermal budgets were chosen to be compatible with deep submicron CMOS processes. Diffusion of dopants is different for GeSi alloys, B diffuses significantly more slowly and As has a much faster diffusion in GeSi. For B doped samples both electrical activation and mobility are higher compared to poly-Si. Also for the first time, data of BF_2^+ doped layers are presented, these show the same trend as the B doped samples but with an overall higher sheet resistance. For arsenic doping, activation and mobility are lower compared to poly-Si, resulting in a higher sheet resistance. The dopant deactivation due to long low temperature steps after the final activation anneal is also found to be quite different. Boron-doped GeSi samples show considerable reduced deactivation whereas arsenic shows a higher deactivation rate. The electrical properties are interpreted in terms of different grain size, quality and properties of the grain boundaries, defects, dopant clustering, and segregation, and the solid solubility of the dopants.

Introduction

Polycrystalline-Ge_xSi_{1-x} is an interesting gate material for sub-0.25 μm complementary metal oxide semiconductor (CMOS) processes.[1] By varying the Ge fraction the work function can be manipulated by 200 to 300 mV toward midgap direction. Furthermore, enhanced dopant activation at low temperatures[1,2] has been observed. This reduces gate depletion, which is extremely important for future CMOS processes. Hence, poly-GeSi can become of importance for future deep submicron CMOS devices, especially for so-called steep retrograde well and ground plane device concepts.[3] Recently, GeSi material has been studied in detail for low temperature thin film transistor (TFT) applications.[4] However, relatively little work has been reported on material properties of poly-GeSi alloys for process conditions compatible with deep submicron CMOS processes.

In this paper, properties of low-pressure chemical vapor deposition (LPCVD) deposited poly-Ge_xSi_{1-x} material are studied for process conditions and temperature budgets compatible to sub-0.25 μm CMOS. A thorough investigation of the morphology, dopant diffusion, and electrical deactivation of B^+, BF_2^+, and As^+ doped poly-$Ge_{0.35}Si_{0.65}$ alloys is presented. It has been found that both p-doped and n-doped poly-GeSi behave considerably differently than reference poly-Si samples. This can be attributed to the different properties of grain boundaries in poly-GeSi which causes a difference in potential barrier energy between GeSi and Si. The p-type nature of traps cause a shift in the energy of the grain boundary trapping states leading to more traps in n-type doped GeSi and a reduction of traps in p-type GeSi compared to poly-Si. This causes the potential barriers in GeSi to be higher for n-type dopants and lower for p-type dopants compared to Si. In the case of As^+ doped films, the enhanced clustering of atoms and segregation of arsenic toward the grain boundaries in GeSi samples causes reduced electron concentrations and higher sheet resistance compared to Si. At very high dopant concentrations the higher solid solubility of boron and the lower solid solubility of arsenic are the main cause of the difference in electrical behavior between GeSi and Si. Boron diffusion is slower in GeSi and the diffusion of arsenic is more rapid in GeSi films, a trend also observed in monocrystalline material. For both p-type and n-type impurities the difference in activation and diffusion compensate giving comparable gate depletion results as poly-Si samples. Although there are differences, for heavily doped samples, no substantial drawbacks for application in CMOS processes have been found.

Experimental

The experiments can be split into two sets, first the diffusion experiments and second the Hall measurements to study the electrical activation. The samples for the diffusion experiments were deposited on thermally oxidized 150 mm (100) Si wafers in the vertical low-pressure chemical vapor deposition (LPCVD) reactor of an ASM Advance 600/2 cluster tool. The poly-Si and poly-$Ge_{0.28}Si_{0.72}$ layers were deposited directly on the SiO_2 layer at deposition temperatures of 620 and 460°C respectively, using silane (SiH_4) and germane (GeH_4) as reactive gases. GeSi deposited at 620°C shows very rough layers and cannot be used. The reduced deposition temperature of 460°C for GeSi deposition is used in order to obtain smooth layers. In addition, the catalytic enhancement of the growth rate in the presence of Ge[5] results in an acceptable growth rate. The layer thickness was 200 nm and the samples were implanted with either $5 \cdot 10^{15}$ BF_2^+ at 20 keV or $5 \cdot 10^{15}$ As^+ at 60 keV. Small dies cut from the wafers were rapid thermally annealed (RTA) for 30 s in N_2 ambient at temperatures between 700 and 900 or 1000°C for BF_2^+ and As^+ implanted layers, respectively. The Ge content of the layers was 28%, determined with Rutherford backscattering spectroscopy (RBS).

The samples for the Hall measurements were grown in a conventional horizontal hot wall LPCVD reactor using SiH_4 and GeH_4 as reactive gasses. The polycrystalline films were deposited on 100 nm thick layers of thermally grown oxide. The deposition temperature was 625 and 500°C for the poly-Si and poly-$Ge_{0.35}Si_{0.65}$, respectively, the latter being chosen because it is the lower limit of the deposition equipment. For these samples the Ge content was determined with energy dispersive x-ray (EDX) analysis, this method was calibrated with RBS data.[5] The following samples were prepared: 500 nm thick layers implanted with $5 \cdot 10^{13}$ to $5 \cdot 10^{15}$ cm^{-2} B^+ at 70 keV, 300 nm thick samples implanted with $5 \cdot 10^{14}$ to $5 \cdot 10^{15}$ cm^{-2} BF_2^+ at 40 keV,

* Electrochemical Society Active Member.

and 300 nm thick layers implanted with $5 \cdot 10^{14}$ to $1 \cdot 10^{16}$ cm^{-2} As^+ at 100 keV. The polycrystalline layers were deposited on (100) Si wafers which were thermally oxidized in dry O_2 to an SiO_2 thickness of 100 nm. The dopant activation was done by furnace anneal at a variety of temperatures. The first 3 min of the anneal were in O_2 ambient followed by an anneal in N_2 ambient except for the 5 min anneals used for the boron doped samples, these received only 1 min of O_2 anneal. The goal of the initial O_2 anneal was to create a thin SiO_2 layer which could retard outdiffusion during the N_2 anneal.

Cloverleaf van der Pauw structures[6] were etched in order to measure Hall mobility and dopant activation in a 0.1 to 1.2 T magnetic field. One of the difficulties with interpreting Hall measurements is that the measured Hall mobility and Hall carrier concentration differ from the electron (or hole) mobility, μ_{drift}, and concentration by a factor r_H, the Hall scattering factor, giving

$$\mu_{drift} = \mu_{Hall}/r_H$$

and [1]

$$n = n_{Hall} \cdot r_H$$

where n (cm^{-3}) is the carrier concentration. The Hall scattering factor r_H is unknown for poly-Si and poly-GeSi but for very high doping concentrations r_H of polycrystalline material will approach the scattering factor for monocrystalline material. For very high magnetic fields ($\mu B >> 1$) it will go toward unity, but for a mobility of $\mu = 10$ cm^2/V s this would require at least a magnetic field of 1000 T, so the scattering factor could not be determined experimentally. For monocrystalline Si this factor is found to be concentration dependent. For doping levels of 10^{18} and 10^{20} cm^{-3}, respectively, r_H between 0.8 and 0.67 has been reported for p-type doped material.[7] For n-type doped layers[8] the scattering factor in Si varies from 1.3 at 10^{18} to 0.9 at 10^{20} cm^{-3}. Manku *et al.*[9] have reported that for p-type doped monocrystalline GeSi the alloy scattering can be neglected in which case the scattering factor for GeSi alloys can be assumed equal to that for Si. Note that all presented data in this work have not been corrected for the Hall scattering factor.

The Hall measurements were performed using a 0.1 to 1.2 T magnet, to determine the sheet resistance, Hall mobility, and the Hall carrier concentration. Arsenic segregation to the grain boundaries was determined for the As^+ doped samples with the highest concentrations by EDX in a high resolution transmission electron microscope (HR-TEM) setup. By focusing the elliptically shaped beam on a grain boundary and subsequent shifting of the beam toward a position inside the grain, an indication of As segregation is obtained. The width of the beam is estimated to be ten times larger than the actual grain boundary, significantly smaller than the grain size. The values of the EDX data are merely a qualitative indication and a lower limit to the As segregation, the exact number of segregated atoms could not be determined. The error in the measurement itself is at most 15%. We used secondary ion mass spectroscopy (SIMS) to determine the diffusion behavior of 20 keV BF_2^+ and 60 keV As^+($5 \cdot 10^{15}$ atom/cm^2) implanted in poly-Si and -$Ge_{0.28}Si_{0.72}$ samples, annealed in an AG Associates 610 Heatpulse with tungsten-halogen lamps RTA setup, in N_2 ambient for 30 s between 700 and 1000°C. The samples were placed on a Si susceptor to assure a constant heat transfer.

Results and Discussion

Physical properties.—The deposition conditions for the samples for the diffusion experiments were optimized to give a smooth surface, as determined with SEM. This yielded for the above described deposition conditions in a texture in between [111] and [220] orientation for the Si sample. The GeSi sample showed a weak [111] orientation. The [311] and [004] peaks were not observed.

Both the $Ge_{0.35}Si_{0.65}$ and the Si samples for the Hall measurements show as deposited a [220] preferential orientation. Small [111] and [311] peaks were observed in the θ to 2θ scans. Despite tilting the sample, the [004] orientation was not measurable. The growth conditions were chosen to obtain smooth layers, having approximately the same grain size as observed from SEM micrographs. Note that the grain size cannot be accurately determined from SEM. In the B^+ doped samples the grain size was slightly larger than in the BF_2^+ and As^+ doped samples because of the larger layer thickness of the B^+ doped samples. The Si samples for the Hall experiments after implantation and anneal show no differences in their XRD-spectrum for all impurity species. The GeSi Hall samples with B^+ and BF_2^+ shows a reduced [111] peak whereas the As^+ doped sample shows an increased [111] peak. In total, after implantation and anneal, the dominant orientation remains [220] for both p-type and n-type doped GeSi and Si after applying the correction factors needed for accurate determination of the texture from the peak heights.[10] In Table I the average grain size of some of the samples is given determined from planar view TEM micrographs. In general, the grain size is larger for GeSi than for Si samples, and larger for n-type doped than for p-type doped samples. Cross-sectional TEM pictures show columnar grains for all samples. After the implantation and anneal the grain sizes show a considerable difference both between Si and GeSi and between the p-type and n-type dopant species.

Diffusion properties.—Dopant diffusion and redistribution is important for interpretation of material properties as well as the electrical characterization of devices. For instance, gate depletion caused by a low concentration of carriers at the gate-SiO_2 interface can be caused by a too low activation level at the poly-oxide interface because the implanted atoms have not diffused to the interface to an adequate level. In Fig. 1 the boron profiles are shown for $5 \cdot 10^{15}$ cm^{-2}, 20 keV BF_2^+ implanted poly-Si and poly-$Ge_{0.28}Si_{0.72}$ as determined by SIMS measurements. For poly-$Ge_{0.28}Si_{0.72}$ the as-implanted boron profile is depicted along with the distribution after 30 s 700, 850, and 900°C RTA anneal in N_2 ambient. For poly-Si the B-profiles after 30 s 700, 800, and 900°C are shown. It appears that the diffusion of boron in poly-GeSi is significantly slower than that in poly-Si. Comparing the SIMS profiles of Fig. 1 it can be seen that the profile in poly-Si after a 30 s 800°C anneal shows enhanced diffusion compared to poly-$Ge_{0.28}Si_{0.72}$ after 30 s 850°C. In both cases for boron doped samples the anneal at 900°C is sufficient to give a nearly flat doping profile.

The diffusion of arsenic doped samples ($5 \cdot 10^{15}$ cm^{-2}, 60 keV) can be observed from Fig. 2. Simultaneous RTA anneals of the GeSi and Si samples of 30 s at 700, 800, 900, and 1000°C, respectively, show clearly the more rapid diffusion of As in $Ge_{0.28}Si_{0.72}$ than in Si. Note that out-diffusion to the N_2 ambient starts at the highest anneal temperature showing the necessity of a capping layer to prevent outgassing which was not used here. The lower concentration found for the GeSi sample might be caused because we used the same matrix factors to calculate the sputter yield as for the poly-Si sample. Another problem is that it is difficult to distinguish As^+ and GeH^+, that can form when some water vapor is left in the vacuum chamber. To double check, we repeated the experiment for 700°C anneal on a different sample which yielded a total of $4.5 \cdot$

Table I. Average grain size of several poly-Si and poly-$Ge_{0.3}Si_{0.7}$ samples determined from planar view TEM micrographs.

Impurity	Grain size (nm)	
	$Ge_{0.35}Si_{0.65}$	Si
$1 \cdot 10^{18}$ cm^{-3} B, 5 min 950°C	76	62
$1 \cdot 10^{20}$ cm^{-3} B, 5 min 950°C	124	80
$1.7 \cdot 10^{20}$ cm^{-3} As, 30 min 950°C	250	126

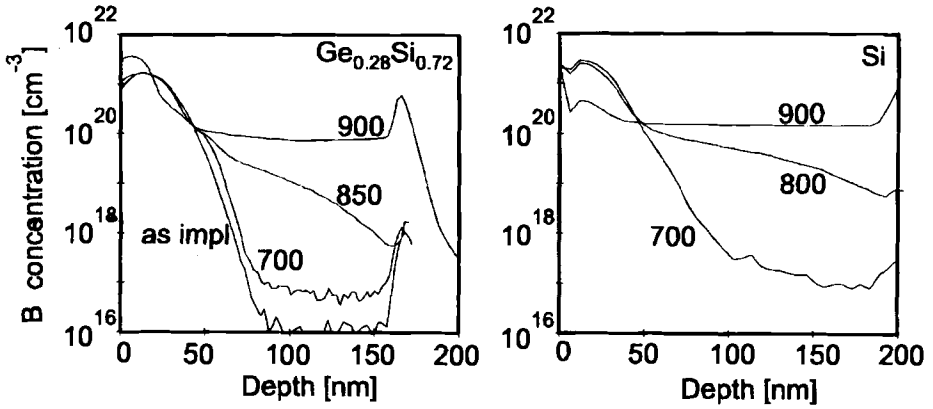

Fig. 1. SIMS diffusion profiles of $5 \cdot 10^{15}$ cm^{-2} BF_2^+ doped poly-$Ge_{0.28}Si_{0.72}$ and poly-Si after 30 s anneals at various temperatures.

10^{15} cm^{-2} arsenic, which is approximately the same yield as in the poly-Si sample, indicating that there seems to be no significant loss in dopants. The erroneous concentrations of the original experiment cannot be explained but it indicated that care must be taken doing these measurements.

Discussion of the diffusion properties.—The diffusion constant can be determined from the diffusion profile under constant total dopant assumption. In the simple model assuming a Gaussian profile and constant total concentration, the concentration is given by

$$C(x, t) \sim \exp(-x^2/4Dt) \quad [2]$$

were C (cm^{-3}) is the dopant concentration, x (cm) is the diffusion depth, D (cm^2/s) is the diffusion coefficient, and t (s) is the anneal time. By plotting the concentration in a semilogarithmic plot against the square of the (sputter depth-projected range), the diffusion constant can be extracted after correcting for the as-implanted profile. For the data under investigation, the maximum concentration is above the solid solubility, where hardly any diffusion takes place, so such a semilogarithmic plot will give several slopes for the different regimes. The diffusion constants presented here are the values in the tail region of the dopant profile.

For the boron doped GeSi sample at 850°C, the diffusion coefficient $D = 3 \cdot 10^{-13}$ cm^2/s, for boron doped poly-Si, annealed at 800°C $D = 8 \cdot 10^{-13}$ cm^2/s. The poly-Si data is in fairly good accordance with results reported by Suzuki *et. al.*[11] considering the possible error on the RTA temperature, possible differences in grain size and processing history and the very rough approximations made here. For the 900°C anneal only a lower limit to the diffusion constant can be determined because of the almost flat profile. The lower limit for both materials is given by $D = 5 \cdot 10^{-12}$ cm^2/s. To determine D more accurately thicker poly layers in combination with a variation in diffusion times would be necessary. The lower diffusion constant of boron in GeSi was already observed for strained layers. Kuo *et al.*[12] have shown a decreasing boron diffusivity with increasing Ge content (up to 20% Ge), and practically no dependence on biaxial strain. The lower diffusion constant of boron in GeSi is not a problem with the temperature budgets used in this study and for current CMOS thermal budgets, but it could become a severe problem if the anneal temperatures are significantly reduced. For RTA anneals the temperature range necessary for good dopant activation is 950 to 1100°C. Since this temperature range will provide a flat doping profile the diffusion of boron is not a limiting factor for CMOS processing.

From Fig. 2 the diffusion coefficient of arsenic in GeSi at 800°C was found to be $D = 3 \cdot 10^{-13}$ cm^2/s. For the higher temperatures and for all the profiles in poly-Si no accurate diffusion coefficient could be determined either because of hardly any change in the profile or an almost flat profile. It has been reported that the diffusivity of As in bulk Ge close to the melting point, T_m, is two orders of magnitude larger than that in bulk Si[13] at T_m. If a linear interpolation would be taken for GeSi the diffusivity in unstrained bulk material would be higher at T_m. Of course any given anneal temperature will be closer to the melting point of GeSi than of Si, so in bulk material the diffusivity is expected to be higher, a trend we also observed in polycrystalline layers. In poly-GeSi the higher diffusion of arsenic might also be caused by the faster recrystallization of the damaged top layer.[14]

The higher diffusivity of arsenic in poly-GeSi compensates for the lower dopant activation in the case of arsenic implantation (see below), giving acceptable gate depletion.[15] For practically used temperature budgets in CMOS, no problem can be expected, as was the case for boron doped samples.

In summary, boron diffuses significantly slower in poly-$Ge_{0.28}Si_{0.72}$ than in poly-Si, whereas arsenic diffuses more rapidly in poly-$Ge_{0.28}Si_{0.72}$. The difference in diffusion

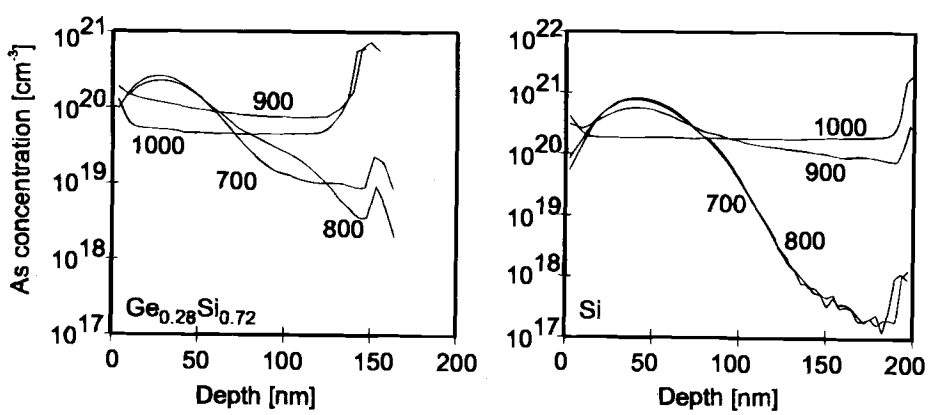

Fig. 2. SIMS diffusion profiles of $5 \cdot 10^{15}$ cm^{-2} As^+ doped poly-$Ge_{0.28}Si_{0.72}$ and poly-Si after 30 s anneals at various temperatures.

already observed for p-type monocrystalline material also exists for the polycrystalline materials studied here. For practically used thermal budgets for CMOS the diffusion is adequate.

Electrical activation.—Boron-doped samples.—In Fig. 3 the results of the Hall measurements (not corrected with r_H) are shown for a range of boron concentrations after a furnace anneal at 800°C for 60 min. This temperature budget ensures a flat dopant diffusion profile. On the horizontal axis the dopant concentration as calculated from the implantation dose is shown. The Hall measurements show a lower sheet resistance of poly-$Ge_{0.35}Si_{0.65}$ over the entire boron concentration range, which is caused by a higher hole mobility and a higher dopant activation. Also shown are the results for BF_2^+ doped samples with the higher doping concentrations (10^{19} to 10^{20} cm^{-3}), having the same general trend as the B^+ doped samples.

Figure 4 shows the sheet resistance, Hall mobility, and percentage of dopant activation after an anneal of 5 min 950°C. Upon this changed thermal treatment the sheet resistance decreases for both poly-Si and poly-GeSi over the entire boron (B^+ and BF_2^+) concentration range. The lowest concentration shows a large increase in activation accompanied by a decrease in mobility for the poly-Si sample compared to the 800°C anneal. The GeSi sample shows a small increase in activation at the same mobility, indicating that the maximum of activation has been almost achieved with the lower anneal temperature. For the higher concentrations the mobility shows little change for both Si and GeSi. The 950°C anneal leads to a higher activation over the entire concentration range. Note that in the case of the highest boron doped layers Hall measurements yield a Hall activation of more than 100% because these data have not been corrected with the Hall scattering factor r_H. If the scattering factor for mono-Si[7] is used for both materials (see experimental) the activation of the highest doped GeSi samples at a prolonged anneal at 950°C comes close to 100% indicating that this scattering factor is a reasonable first order estimation. This is also supported by the fact that the gate depletion for poly-Si and poly-$Ge_{0.35}Si_{0.65}$ gates measured on MOS capacitors is in reasonable accordance with simulations.[16] Therefore we also assume r_H to be equal for B^+ and BF_2^+ doped samples.

To determine the barrier heights of the grain boundary traps, E_b, and the number of traps per unit area, N_T, the sheet resistance has been determined as a function of the measurement temperature for poly-Si and -$Ge_{0.35}Si_{0.65}$ samples annealed for 60 min at 800°C. In Fig. 5 the logarithm of the normalized sheet resistance is plotted as a function of reciprocal temperature, showing a well-defined activation energy that decreased with increasing dopant concentration and that is lower for the GeSi samples compared to the Si samples at equal dose. The values of the barrier energies and the trap densities are given in Table II.

Another important aspect is dopant deactivation during a low temperature process following the final activation anneal. For example an LPCVD TEOS isolation layer is usually deposited at temperatures around 750°C, a temperature at which dopant deactivation can take place. In Fig. 6 the deactivation is shown of $5 \cdot 10^{15}$ cm^{-2} doped samples after a 5 min 950°C anneal and subsequent anneal at 750°C of up to 60 min. The boron doped poly-Si sample shows far more deactivation, 42%, than the $Ge_{0.35}Si_{0.65}$ (23%). Surprisingly the mobility of both samples shows an increase of approximately 17%. If the initial anneal is repeated the sheet resistance returns to its original value. The BF_2^+ doped samples show a similar result with slightly enhanced deactivation for poly-Si. Note that the Hall scattering factor was assumed constant during this experiment. From literature we estimate the error on the r_H with the dopant concentration in this range is 10%.[7] The deactivation in percentages are correct within 10% error margin even in the case that the assumption of equal r_H for both materials should not be correct. Hence poly-GeSi shows significant lower dopant deactivation which is advantageous for future processes that require ultrahigh dopant activation.

Discussion of the B^+ and BF_2^+ materials.—Since boron does not segregate toward the grain boundaries, the electrical behavior of boron doped polycrystalline samples can be explained by the carrier trapping model.[17,18] This model states that electrically active trapping states at the grain boundaries trap carriers, resulting in a potential barrier which blocks the transport of free carriers between the grains, thus reducing the carrier mobility. At low dopant concentrations adding more carriers will increase the potential barrier. When the concentration increases above a critical value, N^*, all traps are filled and additional carriers will decrease the potential barrier and neutral

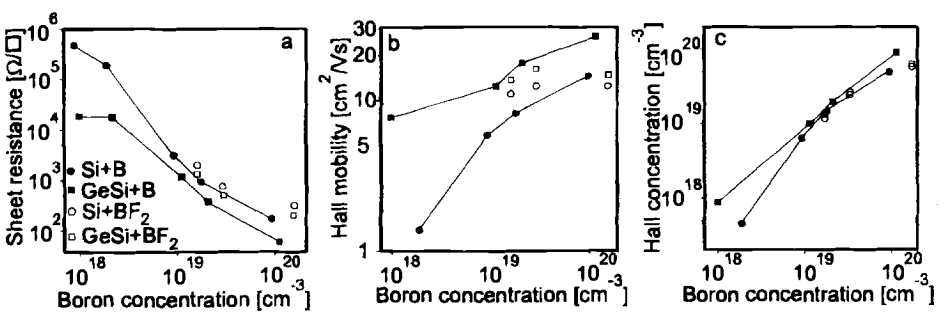

Fig. 3. Sheet resistance (a), Hall mobility (b), and Hall concentration (c) as a function of boron concentration for 500 nm thick B^+ doped and 300 nm thick BF_2^+ doped poly-$Ge_{0.35}Si_{0.65}$ and poly-Si films after 60 min 800°C furnace anneal.

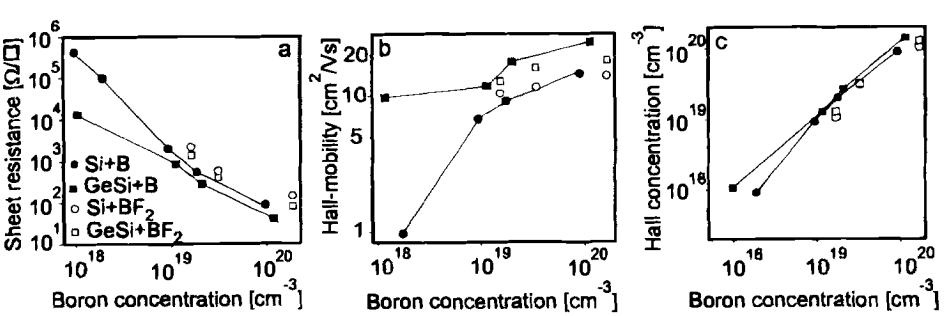

Fig. 4. Sheet resistance (a), Hall mobility (b), and Hall concentration (c) as a function of boron concentration for 500 nm thick B^+ doped and 300 nm thick BF_2^+ doped poly-$Ge_{0.35}Si_{0.65}$ and poly-Si films after 5 min 950°C furnace anneal.

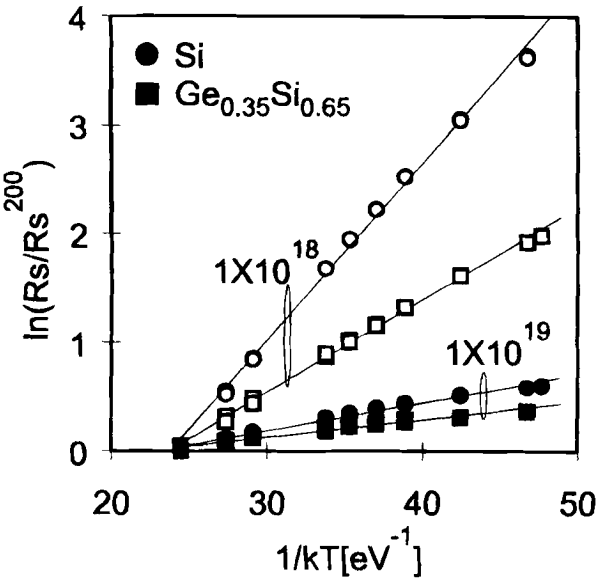

Fig. 5. Normalized sheet resistance (to R_s at 200°C) at varying substrate temperatures for two boron concentrations in poly-$Ge_{0.35}Si_{0.65}$ and poly-Si.

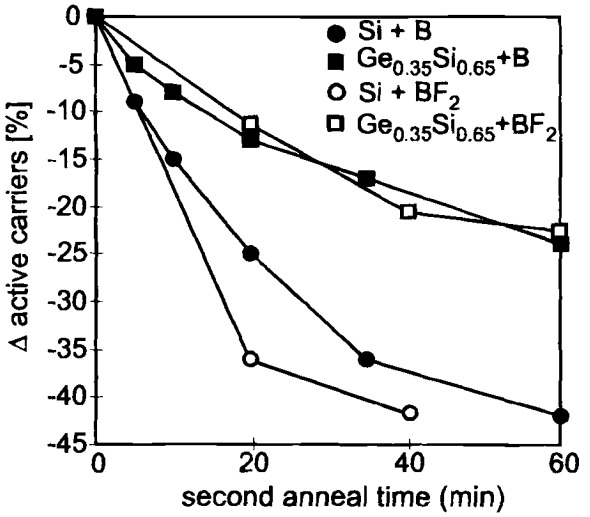

Fig. 6. Percentage of boron deactivation, of $5 \cdot 10^{15}$ cm^{-2} doped layers after an anneal of 5 min 950°C followed by a second anneal of t min 750°C.

regions will form in the grains. The critical dopant concentration depends on the number of traps per unit area N_T (cm^{-2}) and the grain size L (cm)

$$N^* = N_T/L \quad [3]$$

For $5 \cdot 10^{12}$ cm^{-2} traps, a typical value for N_T,[9] and a grain size on 50 nm the critical concentration is $N^* = 10^{18}$ cm^{-3}, so all samples used in this study can be assumed to lie in the range where the potential barrier decreases with increasing dopant concentration. In the case of poly-Si both p-type and n-type doped material will show a similar trapping behavior. In the case of poly-Ge the traps at the grain boundaries are p-type, the energy levels of the traps shift toward the valence band, so that barriers only form in n-type doped material.[19] It is likely GeSi shows a behavior in between the two, with a lower potential barrier for the boron doped samples. In Fig. 3 and Fig. 4 we can see that for the most lowly doped samples the sheet resistance of poly-Si is much higher than that of the GeSi sample, mainly caused by a lower Hall mobility. From the Arrhenius plot of Fig. 5 we determined the barrier energy E_b (eV) and the trap density per unit area of the grain boundary material, N_T (cm^{-2}), for two dopant concentrations using

$$R_s \sim \exp(E_b/kT) \quad [4]$$

and

$$E_b = qN_T^2/8\epsilon N \quad [5]$$

Table II. Grain boundary energy barriers (E_b) and density of trapping states (N_T) of boron doped poly-Si and poly-$Ge_{0.3}Si_{0.7}$ samples for two concentrations. N_T is calculated using both the dielectric constant for Si and an average between the value for Si and Ge.

Sample	E_b (eV)	$N_T(\epsilon = \epsilon_{Si})$ (cm^{-2})	$N_T(\epsilon = \epsilon_{GeSi})$ (cm^{-2})
Si, $1 \cdot 10^{18}$ cm^{-3} B, 60 min 800°C	0.161	$2.9 \cdot 10^{12}$	—
GeSi, $1 \cdot 10^{18}$ cm^{-3} B, 60 min 800°C	0.085	$2.1 \cdot 10^{12}$	$2.2 \cdot 10^{12}$
Si, $1 \cdot 10^{19}$ cm^{-3} B, 60 min 800°C	0.026	$3.7 \cdot 10^{12}$	—
GeSi, $1 \cdot 10^{19}$ cm^{-3} B, 60 min 800°C	0.016	$2.9 \cdot 10^{12}$	$3.1 \cdot 10^{12}$

where N (cm^{-3}) is the acceptor concentration, k is the Boltzmann constant, and ϵ is the dielectric constant of the material. For GeSi both $\epsilon_{Si} = 11.7$ and the weighted average between Si and Ge ($\epsilon_{GeSi} = 13.3$) were used to calculate N_T from the barrier heights. The obtained values for E_b and N_T are listed in Table II. For both dopant concentrations the trap density in Si is larger than in GeSi, and the assumption of all concentrations being above the critical concentration N^* is valid with these trap densities.

The mobility depends linearly on the grain size and exponentially on potential barrier height, it can be expressed as

$$\mu \sim (L/kT) \exp(-E_b/kT) \quad [6]$$

The difference in grain size L (see Table I) between GeSi and Si can account for approximately a factor of 1.5 in mobility. The difference in the barrier energy E_b can lead to a factor 19 difference in mobility for $N = 1 \cdot 10^{18}$ cm^{-3}. Because of the very high sheet resistance of the poly-Si sample at $N = 1 \cdot 10^{18}$ cm^{-3} we were not able to perform an accurate Hall measurement for this sample but extrapolating the data as measured, the difference in mobility can be explained by the larger grain size and the lower potential barrier for the boron doped GeSi sample. The lower Hall concentration for the Si sample can be attributed to the filling of the traps, an effect that becomes relatively less important at higher implantation doses, where the curves approach each other. For the concentrations around $N = 10^{19}$ cm^{-3} not only the active carrier concentrations approach each other also the mobilities come closer together. For both materials the potential barriers are lower with increasing dopant concentration and the relative difference becomes smaller, so that the effect of the potential barriers becomes less important. At a boron concentration of $N = 1 \cdot 10^{19}$ cm^{-3} both the grain size and the barrier difference each contribute to approximately a factor 1.5 difference in mobility giving a mobility that is approximately 2.5 times larger for poly-GeSi. This is consistent with the measurements in Fig. 3 and Fig. 4.

In the highest dopant regime under study, the activation of poly-$Ge_{0.35}Si_{0.65}$ becomes significantly higher than that of poly-Si. Comparing the percentages of activation after 60 min 800°C from Fig. 3, at $N = 2 \cdot 10^{19}$ cm^{-2} we find 93 and 82% for GeSi and Si, respectively. At $N = 1 \cdot 10^{20}$ cm^{-2} the activation is 78 and 50%, respectively. The optimum in the activation can be explained assuming that at the highest dopant concentrations the solid solubility is surpassed. Comparing Fig. 3 and Fig. 4, we find that the higher anneal temperature gives a higher dopant activation for all dopant concentrations. The 5 min 950°C annealed samples give an

activation for $N = 2 \cdot 10^{19}$ cm^{-3} of 123 and 113% for GeSi and Si, respectively, and for $N = 10^{20}$ cm^{-3} this is 116 and 95%, respectively. The larger than 100% activation can be explained because these data are not corrected for the Hall scattering factor, as mentioned before.

After a 5 min anneal at 950°C (Fig. 4) the activation of boron at $N = 1 \cdot 10^{20}$ cm^{-3} shows relatively less decrease when compared to $N = 2 \cdot 10^{19}$ cm^{-3}, than the samples annealed at 800°C, presented in Fig. 3. This is in accordance with the fact that the solid solubility of boron increases with increasing temperature. From our data, after correcting with the scattering factor, we extract the solid solubility for the GeSi sample at 800 and 950°C anneal respectively $6 \cdot 10^{19}$ cm^{-3} and $9 \cdot 10^{19}$ cm^{-3}. The solid solubility of the Si samples are $3 \cdot 10^{19}$ cm^{-3} at 800°C and $6 \cdot 10^{19}$ cm^{-3} at 950°C. The values for the solid solubility of boron in poly-Si we have obtained are in good accordance with results of Suzuki *et. al.*[20] who found $6 \cdot 10^{19}$ and $1.5 \cdot 10^{20}$ cm^{-3} at 800 and 1100°C, respectively, using Hall measurements without correction factor. For single-crystalline Ge the melting point distribution coefficient of boron is a factor 2 larger than that in Si,[21] a quantity that is linked to the solid solubility. The value for GeSi will lie in between the two values at the melting point. The observed trend in polycrystalline material is therefore the same as in bulk material.

The BF_2^+ doped samples show the same general behavior as the B doped samples, having a slightly higher sheet resistance due to the difference in layer thickness. The mobility of BF_2^+ doped samples might be different because of a difference in grain size due to the amorphization of the top layer. The presence of large amounts of fluorine in the material might limit the mobility and could influence the solid solubility of boron, but further research is needed to fully explain the difference between the two p-type dopant species.

The deactivation measurement presented in Fig. 5 of the $5 \cdot 10^{15}$ cm^{-2} doped samples is additional proof that the solid solubility of boron in GeSi is higher than in poly-Si samples. The increase in mobility of about 17% means that once the traps at the grain boundaries are filled the deactivation anneal does not affect the number of filled traps and the energy barriers at the grain boundaries. The mobility is enhanced because of the reduction of charged scattering centers, for example by the forming of neutral clusters of boron. The rate of deactivation is higher for poly-Si, this can be attributed to the difference in diffusivity of boron, and therefore the time needed to form neutral clusters. After a 60 min anneal at 750°C the hole concentration is still higher than the hole concentration after a 60 min 800°C anneal as seen in Fig. 3. This means that the maximum deactivation until the solid solubility level at 750°C, is not reached in 60 min. For practical use in CMOS technologies the deactivation can be minimized by decreasing the duration of the low temperature step. Even more effective would be decreasing the temperature at which the LPCVD TEOS layers are deposited since the diffusion of the dopants influences the rate of deactivation.

In summary, the change in the position of the energy levels of the grain boundary traps toward the valence band in poly-GeSi make the potential barriers lower. As a result a higher mobility for boron doped poly-GeSi samples is found. This effect is most important at the lowest dopant concentrations. At higher concentrations the difference in grain size plays a role. The dopant activation of poly-Si is limited for very low dopant concentrations because of the increased trap density compared to GeSi. In the medium concentration regime under study the activation is similar for both materials and for the highest concentrations the higher solid solubility of boron in poly-GeSi increases the Hall concentration significantly when compared to poly-Si. The trend for the BF_2^+ doped samples is the same, the main difference is the higher sheet resistance due to the difference in layer thickness.

Arsenic doped samples.—Figure 7 shows the results of the Hall experiments on arsenic doped layers, which were furnace annealed for 30 min at 950°C. An increase in the sheet resistance and a decreasing dopant activation for GeSi samples compared to the Si reference samples is observed. Also, a decrease in the Hall electron mobility for GeSi samples is found. Preliminary results on phosphorous doped samples show similar results, in contrast to results presented by King *et al.*[2] Here n-type doped GeSi shows an increase in mobility and dopant activation up to a Ge content of 35%.

In Fig. 8 the results are shown for 60 min anneals at varying temperatures. The sheet resistance of the $N = 1.7 \cdot 10^{20}$ cm^{-3} doped samples decreases with increasing anneal temperature caused by a linear increase in mobility and an increased dopant activation. The difference between the poly-Si and poly-GeSi sample is most pronounced at the lowest anneal temperature. The $Ge_{0.35}Si_{0.65}$ layers shows an continuous decreasing sheet resistance whereas the poly-

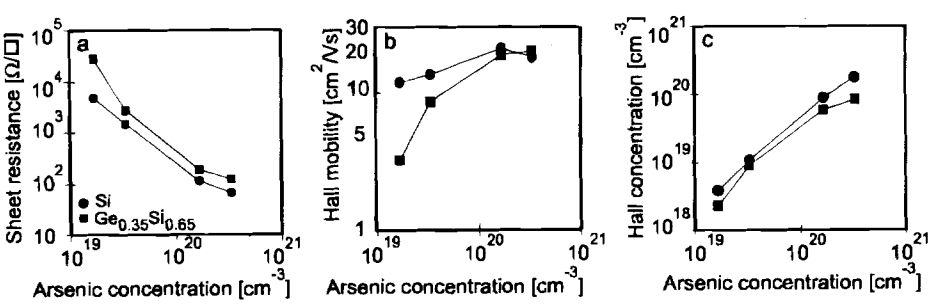

Fig. 7. Sheet resistance (a), Hall mobility (b), and Hall concentration (c) as a function of arsenic concentration for 300 nm thick As^+ doped poly-$Ge_{0.35}Si_{0.65}$ and poly-Si after 30 min 950°C furnace anneal.

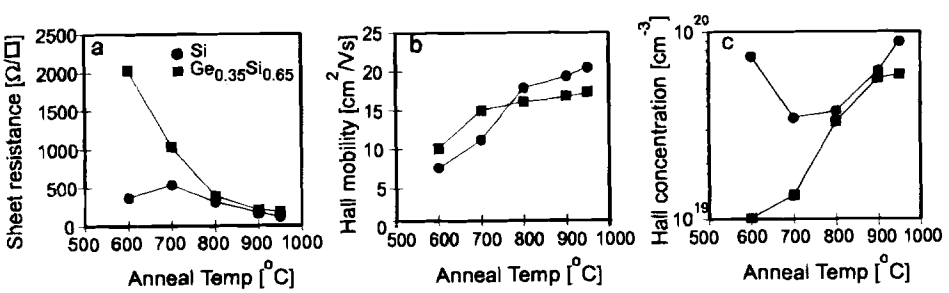

Fig. 8. Sheet resistance (a), Hall mobility (b), and Hall activation (c) for $5 \cdot 10^{15}$ cm^{-2} doped poly-$Ge_{0.35}Si_{0.65}$ and poly-Si after 60 min anneals at various anneal temperatures.

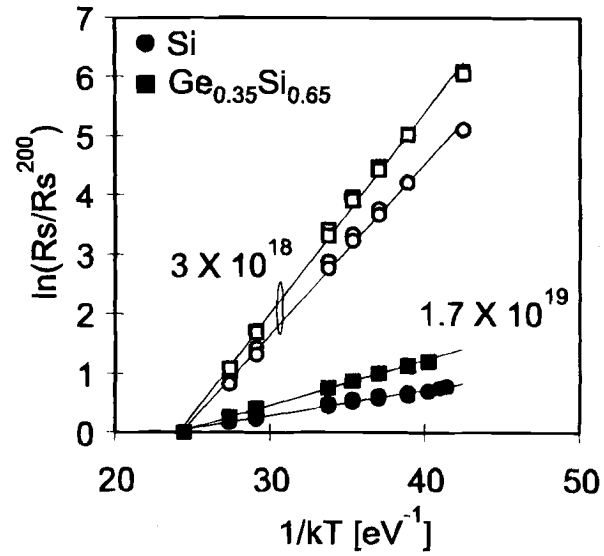

Fig. 9. Normalized sheet resistance (to R_s at 200°C) at varying substrate temperatures for two arsenic concentrations in poly-$Ge_{0.35}Si_{0.65}$ and poly-Si.

Si has a maximum at 700°C, caused by a minimum in the Hall concentration.

In Fig. 9 the logarithm of the normalized sheet resistance is plotted *vs.* the inverse substrate temperature for $3.3 \cdot 10^{18}$ and $1.7 \cdot 10^{19}$ cm^{-3} As^+ doped poly-Si and poly-$Ge_{0.35}Si_{0.65}$ samples. Just as in the case of the boron-doped samples we see a decrease in slope with increasing donor concentration N_d, and thus a lowering of the potential barrier energy. In contrast to boron doped samples the poly-Si samples show a reduced slope and thus a lower E_b than the GeSi samples for both carrier concentrations. The values of the barrier energies and the corresponding trap density N_T are listed in Table III. Data for GeSi are calculated both when applying the dielectric constant for Si and for a weighted average between the values of Si and Ge. It can be seen that the barriers in poly-GeSi are higher and the trap density is considerably larger in the GeSi sample.

Deactivation of dopants when a lower temperature is applied after the final activation step is an important issue for As^+ doped layers in NMOS applications.[22] We have annealed the $N = 3.3 \cdot 10^{20}$ cm^{-3} As doped samples 30 at min 950°C and subsequently up to 65 min at 750°C in N_2 ambient. Figure 10 shows the sheet resistance and the percentage of dopant deactivation of $N = 3.3 \cdot 10^{20}$ cm^{-3} As^+ doped samples. The final percentage of deactivation is about 40% for both poly-Si and poly-$Ge_{0.35}Si_{0.65}$. Note that in the latter case this is already obtained after the first 20 min anneal. Note also that the sheet resistance of the poly-Si sample increases but the poly-GeSi sample shows an almost flat curve for the sheet resistance or better even a slight decrease. The decrease in Hall electron concentration is in both cases accompanied by an increase in electron mobility. For GeSi this increase is much larger, from $\mu = 19.2$ to $\mu = 35.2$ cm^2/Vs, compared to an increase from $\mu = 18.5$ to $\mu = 24.7$ cm^2/Vs for Si. Performing the same experiment on samples with $1.7 \cdot 10^{20}$ cm^{-3} As^+ doping shows the same trend, Si has an increasing sheet resistance caused by deactivation (25%) and showing a small increase in mobility whereas GeSi shows no change in sheet resistance, approximately the same deactivation (30%) and considerably more increase in electron mobility compared to Si.

Table III. Grain boundary energy barriers (E_b) and density of trapping states (N_t) of arsenic doped poly-Si and poly-$Ge_{0.3}Si_{0.7}$ samples for two concentrations. N_t is calculated using both the dielectric constant for Si and an average between the value for Si and Ge.

Sample	E_b (eV)	$N_T (\epsilon = \epsilon_{Si})$ (cm^{-2})	$N_T (\epsilon = \epsilon_{GeSi})$ (cm^{-2})
Si, $3.3 \cdot 10^{18}$ cm^{-3} As, 30 min 950°C	0.289	$7.0 \cdot 10^{12}$	—
GeSi, $3.3 \cdot 10^{18}$ cm^{-3} As, 30 min 950°C	0.341	$7.6 \cdot 10^{12}$	$8.1 \cdot 10^{12}$
Si, $1.7 \cdot 10^{19}$ cm^{-3} As, 30 min 950°C	0.043	$6.2 \cdot 10^{12}$	—
GeSi, $1.7 \cdot 10^{19}$ cm^{-3} As, 30 min 950°C	0.077	$8.2 \cdot 10^{12}$	$8.8 \cdot 10^{12}$

Figure 11 shows the ratio of arsenic atoms at the grain boundary to inside the grain (GB/GR-ratio) determined by means of EDX measurements in an HR-TEM setup. Poly-Si and poly-$Ge_{0.35}Si_{0.65}$ samples doped with $1.7 \cdot 10^{20}$ and $3.3 \cdot 10^{20}$ cm^{-3} arsenic after a 30 min 950°C anneal were investigated. Also shown are the results after deactivation, *e.g.*, 30 min 950°C + 60 min 750°C. The result shows a clearly higher ratio for the GeSi samples compared to Si. Previous experiments on *in situ* doped poly-Si samples with a scanning TEM (STEM)[23] show a ratio of approximately three. Note that the technique used in this work shows a difference between GeSi and Si, but the absolute values of number of segregated As atoms cannot be calculated since the ellipse shaped beam is estimated to be approximately ten times larger than the width of the grain boundary, this means that the actual effect can be ten times larger than the measured ratio. The GB/GR-ratios for the poly-Si samples all vary around 1.1, for the poly-GeSi sample this is significantly larger. The smaller ratio for poly-Si compared to literature[23] is attributed to the spot size of the used electron beam. The effect of deactivation on segregation measured with EDX is shown in the last two columns in Fig. 11. For poly-Si both the ratio after activation and after the subsequent deactivation is approximately one, and no difference can be determined within the error margins of the technique. For poly -GeSi the GB/GR-ratio before (1.7) and after (1.5) the deactivation anneal is also the same, within the error margins of the technique.

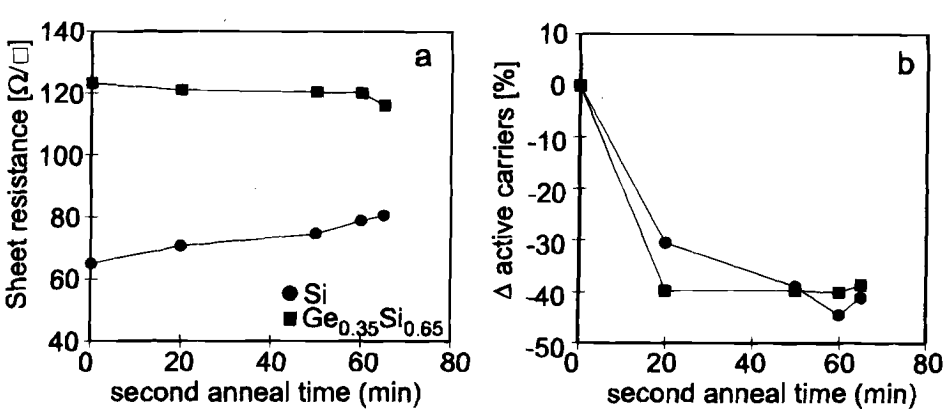

Fig. 10. Sheet resistance (a) and percentage of arsenic deactivation (b), of $1 \cdot 10^{16}$ cm^{-2} doped layers after an anneal of 30 min 950°C followed by a second anneal of *t* in 750°C.

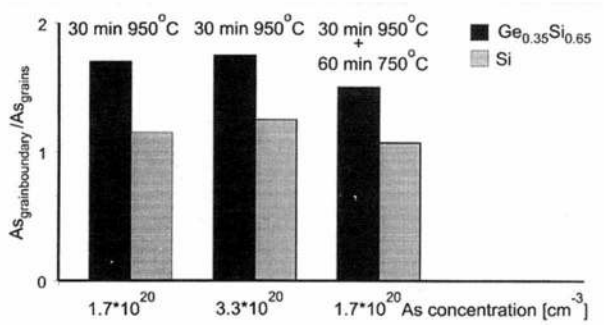

Fig. 11. Ratio of arsenic segregated toward the grain boundaries to arsenic in the grains, determined with EDX.

Discussion of the As⁺ doped materials.—In n-type doped polycrystalline samples both dopant segregation toward the grain boundaries and carrier trapping of the electrons influence the electrical behavior of the samples.[24] In Fig. 7 the increase in Hall concentration with the donor concentration is much larger than for the boron-doped samples. The very low dopant activation, 22 and 13% at $N = 1.7 \cdot 10^{19}$ cm^{-3} and 55 and 35% at $N = 1.7 \cdot 10^{20}$ cm^{-3} in poly-Si and poly-GeSi, respectively, can be attributed to the segregation of As toward the grain boundaries. Since dopant segregation is reduced at higher anneal temperatures the Hall electron concentration increases rapidly with the anneal temperature, as can be seen from Fig. 8. The low sheet resistance and relatively high electron concentration for poly-Si annealed for 60 min at 600°C can be attributed to solid phase epitaxy and the very low diffusion constant at this temperature. Hence only a small amount of As can reach the grain boundaries or cluster and a high electron concentration is observed. The higher diffusivity of As in GeSi causes the Hall concentration at 600°C anneals for the GeSi sample to be very low already, due to segregation. It is likely that solid phase epitaxy in GeSi takes place at lower anneal temperatures, so that a maximum in the sheet resistance might be observed when adding measurements at lower anneal temperatures. The trend in Fig. 7 and Fig. 8 shows the same general behavior for GeSi and Si samples, both indicate that As segregation is applicable.

Not only segregation but also carrier trapping plays a role in the electrical behavior of arsenic-doped films. From Table III we can observe that GeSi samples have an increased potential barrier energy at the grain boundaries and the amount of traps is increased with respect to the Si reference sample. This is caused by a shift in energy level of the grain boundaries traps toward the valence band in n-type doped GeSi. The lowest arsenic concentration, $N = 1.7 \cdot 10^{19}$ cm^{-3} in Fig. 7 shows a much lower Hall electron mobility for GeSi than for Si. Using Eq. 5 and the values for the barrier heights in Table III, we can account for a four times larger electron mobility of Si at this concentration. The increase in mobility and the reduction of the difference between GeSi and Si is due to the decrease of the barrier energy with increasing dopant concentration. Although we do not have grain sizes and barrier energies for all samples the trend seems to be clear. At the lowest concentrations the difference in barrier height is most important and at higher concentrations the effect of the energy barrier difference and the difference in grain size will have an effect in the same order of magnitude, only of opposite sign resulting in equal mobilities for both materials.

At high concentrations the solid solubility of As becomes the limiting factor determining the amount of free electrons. In Fig. 7 for the highest As implantation concentrations the curve for Si is almost linear, whereas for GeSi the concentration saturates indicating that the solid solubility of As is reached in the GeSi sample, and that it is smaller in poly-GeSi than in poly-Si. The bulk solid solubility of As in pure Ge is more than a decade lower than that in Si,[13,21] at the melting point (T_m) and the value for Ge_xSi_{1-x} will probably be in between the data for Ge and Si. We assume that the trend will be the same in polycrystalline materials and the Hall data seem to corroborate this. From Fig. 7 the maximum As concentration in GeSi is found to be $8 \cdot 10^{19}$ cm^{-3} and the kink in the Hall concentration curve indicated that this is the solid solubility for As in GeSi. The maximum As concentration in poly-Si is $2 \cdot 10^{20}$ cm^{-3} which equals the value of the solid solubility in poly-Si reported by others[19] indicating that here also the solid solubility is almost reached.

The EDX measurements in a TEM setup on the highest doped samples presented in Fig. 11 show clearly that the amount of As segregated toward the grain boundaries is significantly larger in poly-$Ge_{0.35}Si_{0.65}$. The deactivation of poly-Si has been attributed previously to arsenic segregation to the grain boundaries, a subsequent high temperature anneal would result in a "desegregation" back into the grain.[25] Our EDX data indicate that changes in segregation are small, this might be caused by restrictions of the resolution of the measurement technique and partially by the fact that at high dopant concentrations the number of dopants that segregate is relatively small compared to the total number of dopant atoms. The very large grains in combination with the low diffusivity at 750°C may also prevent As from segregating to a large extent. The observed electrical deactivation in Fig. 10 can partly be caused by the segregation to the grain boundary. However, the exceeding of the solid solubility of As in Si or GeSi leading to the formation of neutral clusters of arsenic could be more important. Since the deactivation is combined with a large increase in electron mobility, a reduction in the concentration of charged scattering centers is likely. With the resolution of our EDX data we cannot conclude whether or not dopant segregation toward the grain boundaries is an important cause of deactivation. It seems likely that also cluster formation by the exceeding of the solid solubility is an important cause of the deactivation.

In summary, from Fig. 7 and Fig. 8 we can conclude that the difference in activation behavior between poly-$Ge_{0.35}Si_{0.65}$ and poly-Si is probably caused by difference in solid phase epitaxy behavior and a lower diffusivity of As in poly-Si, preventing segregation at 600°C in poly-Si. More segregation of As toward the grain boundaries occurs in poly-GeSi and a lower solid solubility of As in GeSi is found which is of importance for the highest impurity concentrations. The mobility difference is caused by a reduced trap density and a lower energy barrier in poly-Si but this is compensated by the larger grain size at higher dopant concentrations. The grain size is an important factor and might explain the lower sheet resistance for phosphorous doped poly-GeSi compared to poly-Si observed by others.[2]

Conclusions

The electrical properties of poly-GeSi have been studied in detail. We have shown that boron diffuses significantly faster in poly-Si than in poly-GeSi. However, for both materials 30 s at 900°C gives an almost flat doping profile. Hence the reduced diffusion constant does not limit the processing. Arsenic shows an enhanced diffusivity in GeSi and a 30 s at anneal 900°C also provides an almost flat profile. The difference in diffusion is significant but for thermal budgets used in current CMOS processes the diffusion is not a limiting factor.

The shift of the energy levels of the grain boundary trapping states toward the valence band in poly-GeSi causes a reduction in energy barriers and trap density at the grain boundary in p-type doped GeSi compared to Si. For n-type doped GeSi this shift in energy levels causes an increase in barrier height and trap density with respect to Si. This results in a higher hole mobility in p-type GeSi and a lower electron mobility in n-type GeSi with respect to Si. The barrier heights have the largest effect for low dopant concentrations. For intermediate doping concentrations the larger grain size of GeSi samples plays a role. For arsenic-doped GeSi besides the difference in barrier

height also the enhanced segregation of arsenic toward the grain boundaries and cluster formation reduce the Hall electron concentration when compared to the reference poly-Si sample. For very high dopant concentrations, as commonly used in state-of-the-art CMOS processes, the solid solubility of the dopants is the limiting factor in the dopant activation. The solid solubility of boron is larger in GeSi than in Si leading to a higher maximum hole concentration. The solid solubility of arsenic is lower in GeSi than in Si resulting in a lower maximum electron concentration. Applying a reduced temperature will lead to deactivation of dopants. Boron doped Si shows 42% deactivation after 60 min 750°C which is almost twice the percentage of deactivation in GeSi (23%). Arsenic doped Si and GeSi both have 40% deactivation after 60 min 750°C. The rate of deactivation is dictated by the diffusivity of the dopant species so deactivation can be minimized by reducing the time and the temperature of any post activation process steps.

The results presented in this paper show that from the point of view of dopant diffusion and electrical activation no significant problems occur when polycrystalline germanium-silicon alloys are used as gate material for submicron MOS devices. The effect of Φ_{ms} can be exploited for devices and will be reported in another paper.

Acknowledgments

The authors would like to thank the Dutch Technology Foundation (STW) and the Dutch Foundation for Fundamental Research on Matter (FOM) for their financial assistance. Philips Research Laboratories, Eindhoven, The Netherlands, are acknowledged for the use of their cleanroom facilities. R. de Kruif and J. van Berkum are thanked for the SIMS measurements and E. G. Keim of the Center for Materials Research (CMO) for the TEM and EDX measurements. The authors are grateful to J. H. Klootwijk, H. Lifka, J. B. Rem, and J. Schmitz for fruitful discussions.

Manuscript submitted March 10, 1997; revised manuscript received June 24, 1997.

The University of Twente assisted in meeting the publication costs of this article.

REFERENCES

1. T. -J. King, J. R. Pfiester, J. D. Shott, J. P. McVittie, and K. C. Saraswat, in *Tech. Dig. Int. Electron Device Meet.*, 253 (1990).
2. T.-J. King, J. P. McVittie, K. C. Saraswat, and J. R. Pfiester, *IEEE Trans. Electron Dev.*, **ED-41**, 228 (1994).
3. T. Scotnicki, in *Proceedings of ESSDERC'96*, pp. 505-514, (1996).
4. D. S. Bang, M. Cao, A. Wang, and K. C. Saraswat, *Appl. Phys. Lett.*, **66**, 195 (1995).
5. J. Holleman, A. E. T. Kuiper, and J. F. Verweij, *This Journal*, **140**, 1717 (1993).
6. L. J. van der Pauw, *Philips Res. Rep.*, **13**, 1 (1958).
7. Y. Sasaki, K. Itoh, E. Inoue, S. Kishi, and T. Mitsusuishi, *Solid-State Electron.*, **31**, 5 (1988).
8. J. A. del Alamo and R. M. Swanson, *J. Appl. Phys.*, **57**, 2314 (1985).
9. T. Manku, J. M. McGregor, A. Nathan, D. J. Roulston, J. P. Noël, and D. G. Houghton, *IEEE Trans. Electron Dev.*, **ED-40**, 1990 (1993).
10. C. Salm, J. G. E. Klappe, J. Holleman, J. B. Rem, and P. H. Woerlee, *MRS Proc.*, **343**, 721 (1994).
11. K. Suzuki, A. Satoh, T. Aoyama, I. Namura, F. Inoue, Y. Kataoka, Y. Tada, and T. Sugii, *This Journal*, **142**, 2786 (1995).
12. P. Kuo, J. L. Hoyt, J. F. Gibons, J. E. Turner, and D. Lefforge, *Appl. Phys. Lett.*, **66**, 580 (1995).
13. Landolt-Börnstein, *Zahlenwerten und Functionen aus Naturwissenschaften und Technik*, Band 17, Springer Verlag, Berlin (1984).
14. To the knowledge of the authors no extensive studies on the recystallization of arsenic doped poly-GeSi have been performed but phosphorous doped GeSi crystallizes significantly faster than P^+ doped Si. To be published by J. B. Rem *et al.*
15. C. Salm, J. Schmitz, M. C. Martens, D. J. Gravesteijn, J. Holleman, and P. H. Woerlee, *Proceedings of ESSDERC'96*, pp. 601-604 (1996).
16. Unpublished work.
17. J. Y. W. Seto, *J. Appl. Phys.*, **46**, 5247 (1975).
18. G. Baccarani, B. Ricco, and G. Spadini, *ibid.*, **49**, 5565 (1978).
19. T. I. Kamins, *Polycrystalline Silicon for Integrated Circuit Applications*, 2nd ed., Kluwer Academic Publishers, Boston (1988).
20. K. Suzuki, N. Miyato, and K. Kawamura, *Jpn. J. Apl. Phys.*, **34**, 1748 (1995).
21. F. A. Trumbore, *Bell System Tech. J.*, **39**, 205 (1960); and references therein.
22. A. H. Perera, W. J. Taylor, and M. Orlowski, in *Int. Electron Devices Meet. Tech. Dig.*, p. 835 (1993).
23. C. Y. Wong, C. R. M. Grovenor, P. E. Batson, and D. A. Smith, *J. Appl. Phys.*, **57**, 438 (1985).
24. M. M. Mandurah, K. C. Saraswat, and T. I. Kamins, *IEEE Trans. Electron Devices*, **ED-28**, 1163, 1171 (1981).
25. M. M. Mandurah, K. C. Saraswat, and T. I. Kamins, *Appl. Phys. Lett.*, **36**, 683 (1980).